

## Why Are the Structures of Some Solids So Complex but Others So Simple?

Jeremy K. Burdett,\* Carol Marians, and John F. Mitchell†

Department of Chemistry and James Franck Institute, The University of Chicago, Chicago, Illinois 60637

Received November 10, 1993\*

Three different theoretical considerations are used to probe some of the factors which determine the “complexity” of solids. It is first shown how simple topological restrictions, set by stoichiometry and local coordination number, have an important bearing on the generation of locally symmetric arrangements of atoms. Through the introduction of an orbital picture which provides an electronic underpinning of the valence sum rules of Pauling and Brown, it is shown how the local structure is determined by the electronic configuration. Finally, the use of the method of moments enables comments to be made concerning the identity of nearest-neighbor atoms and linkages of various types as a function of electron count. By study of the behavior of the fourth moment as a function of an order parameter, it is shown how ordered arrangements of atoms and bonds are electronically favored.

### Introduction

One of the most striking features of the panoply of structures found in the solid state is their wide range of complexity. The very simple structure of rock salt and the many other systems which may be generated by filling the interstices of close-packed anionic arrays stand in stark contrast to many of the “complex” structures of the mineral world. But what do we mean by “complex”? There is no obvious single parameter which immediately comes to mind. Certainly low symmetry as in crystal class or space group is a useful index, and the presence of atoms in distorted local environments and symmetry inequivalent atoms of the same chemical identity are two other indicators. The latter lead to a large number of atoms in the asymmetric unit and often large unit cells. It is clear though that “complexity” is largely a qualitative, frequently intuitive, notion.

The structure of angelellite,  $\text{Fe}_4\text{As}_2\text{O}_{11}$ , shown in Figure 1, is<sup>1</sup> a simple one compared to many structures, but one where the iron octahedra are distorted so that there are no angles of 90 or 180° and of the FeO distances, no two are the same, a situation very different from that of rock salt. This pair of structures immediately prompts two questions. First, why does angelellite not adopt a much simpler structure and second why does rock salt not adopt a more complex one? A more “complex” structure is indeed found for ZrCl. If the close-packed sheets in NaCl are arranged in the order ...NaClNaClNaClNaCl..., then the sheets in ZrCl are arranged<sup>2</sup> as ...ZrZrClClZrZrClCl.... A similar pair of questions is applicable to the very simple structures found for most of the elemental metals but the frequently very complex arrangements found for the  $\chi$ -phases and alloys such as  $\text{Cu}_4\text{Cd}_3$  (see ref 3). These two questions can be viewed within a wider context. Since one extreme of atomic complexity is associated with the arrangements found in disordered systems, it is pertinent to ask why there are crystals at all. This question, of course, is in two parts. The first asks what are the factors determining long-range order in crystals. (Thus  $\text{Cu}_3\text{Au}$ , for example, is crystalline below 663 K, but above this temperature has no long range order, the Cu and Au atoms being disordered over the sites of the fcc lattice.) The second asks if ordered structures with

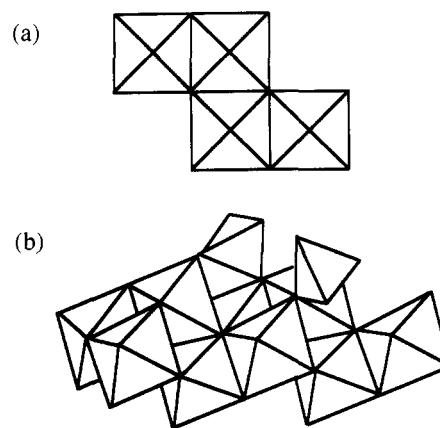


Figure 1. Structure of angelellite:<sup>1</sup> (a) showing the basic building blocks of iron-centered octahedra; (b) showing how chains of such octahedra are linked via arsenic-centered tetrahedra.

small unit cells of high symmetry should be favored over amorphous materials, namely those disordered systems with “complex” cells of infinite size. Recognizing that entropic factors in general stabilize disordered structures, what are the electronic factors which stabilize ordered arrangements of atoms? This is a question which has been of interest for years. Laves argued<sup>4</sup> that atoms, if regarded as objects with a uniform diameter and an incompressible exterior, would be expected to pack together in space to give crystal structures with the highest symmetry, highest coordination numbers, and densest packing of atoms. In fact atoms are not characterless spheres like billiard balls, and there are certainly electronic reasons<sup>5,6</sup> for the stability of such close-packed arrangements.

This article will address some of these questions and is in three parts. The first examines some of the topological restrictions implied by the local coordination and stoichiometry. The second uses traditional orbital ideas and the angular overlap model<sup>7</sup> and the third the more global picture provided by the method of moments<sup>6,8</sup> to make general statements concerning the factors

\* To whom correspondence should be addressed at the Department of Chemistry, University of Chicago.

† Present address: Materials Sciences Division, Argonne National Laboratory, Argonne, IL 60439.

• Abstract published in *Advance ACS Abstracts*, April 1, 1994.

(1) Moore, P. B.; Araki, T. *Neues Jahrb. Mineral., Abh.* 1978, 132, 91.

(2) Corbett, J. D. *Acc. Chem. Res.* 1981, 14, 239.

(3) Pearson, W. B. *The Crystal Chemistry and Physics of Metals and Alloys*; Wiley: New York, 1972.

(4) Laves, F. *Theory of Alloy Phases*; American Society for Metals: Metals Park, OH, 1956.

(5) Lee, S. J. *Am. Chem. Soc.* 1991, 113, 8211.

(6) Burdett, J. K. *Struct. Bonding* 1987, 65, 30.

(7) Burdett, J. K. *Molecular Shapes*; Wiley: New York, 1980.

(8) (a) Cyrot-Lackman, F. *Adv. Phys.* 1967, 16, 393. (b) Lee, S. Acc. Chem. Res. 1991, 24, 249. (c) Pettifor, D. G. In *Electron Theory in Alloy Design*; Pettifor, D. G., Cottrell, A., Eds.; Institute of Materials; London, 1992.

influencing the stability of structures. The focus will exclude molecular structures held together by van der Waals interactions. We begin our discussion with some considerations of Pauling's rules.<sup>9</sup>

### Pauling's Second Rule and the Structure of Angelellite

Pauling's rules<sup>9</sup> were initially assembled to guide the understanding of crystal structures of the "ionic" type, although it is clear that the general ideas are applicable to a wider class of materials. Pauling's first rule introduces the idea of ionic "size" and, via the radius ratio, considerations of local geometry. It is however, the second rule which starts to determine how an extended array is built up. The second rule is usually stated as follows: "In a stable coordinated structure the total strength of the valency bonds which reach an anion from all the neighboring cations is equal to the charge of the anion." In early use of this idea, Pauling envisaged the electrostatic bond strength (ebs) as being equal to the cation charge divided by the coordination number of the cation. As an example, in NaCl each cation is linked to six anions and the ebs of each anion-cation linkage is  $1/6$ . Thus the sum of the ebs of the six bonds to the cation is just  $\sum \text{ebs} = 6 \times 1/6 = 1$ , and the rule is obeyed. This is a simple example, but through its trivality surely indicates that there is strong topological and stoichiometric control behind the operation of the second rule. First, the total anion and cation charges must balance, and second the coordination numbers of anion and cation are related through the stoichiometry. In the general case where there are  $N_{a,c}$  anions and cations with charges  $C_{a,c}$ , and coordination numbers  $\Gamma_{a,c}$ , the ebs of one leg of the cation coordination sphere is  $C_c/\Gamma_c$  and thus

$$\sum \text{ebs} = (C_c/\Gamma_c)\Gamma_a \quad (1)$$

Electrical neutrality ensures that  $N_a C_a = N_c C_c$  and, topological-stoichiometry restrictions means that since each anion is connected to a collection of cations and vice versa,  $N_a \Gamma_c = N_c \Gamma_a$ . This leads to the relationship

$$\sum \text{ebs} = C_c(\Gamma_a/\Gamma_c) = C_c(N_c/N_a) = C_c(C_a/C_c) = C_a \quad (2)$$

Equation 2 shows dramatically the origin of the strong topological-stoichiometric control of the rule. There are some more general arguments which allow somewhat broader statements described by Ellison and Navrotsky.<sup>10</sup> It is clear that arguments such as these allow a ready appreciation of why Pauling's second rule is obeyed in a multitude of systems. The rule though does not hold in many cases. Particularly interesting for us here is to show why it cannot work for the structure found for the mineral angelellite and thus leads to the asymmetrical arrangement found. Could there be other structures for angelellite which do satisfy Pauling's rule and may be of lower energy? Of course we could ask the related question as to whether there are other structures for NaCl which do not satisfy the rule and are of higher energy. Certainly the structures of many systems, molecules, and solids are distorted from a more highly symmetrical parent for reasons which are often simple to understand. The Peierls distortion of the polyacetylene chain and its molecular cyclobutadiene Jahn-Teller analog follow from simple electronic considerations associated with the nature of the highest occupied energy levels of the system.<sup>11</sup> Such mechanisms can be excluded here—these mechanisms are not appropriate for angelellite. It is an insulator. Similarly the "ferroelectric distortion" in  $\text{BaTiO}_3$  is readily understandable<sup>12</sup> in terms of a second order Peierls or Jahn-Teller effect.

The structure of angelellite,  $\text{Fe}^{3+}_4\text{As}^{5+}_2\text{O}_{11}$ , is composed of linked  $\text{Fe}^{3+}\text{O}_6$  octahedra and  $\text{As}^{5+}\text{O}_4$  tetrahedra, each, as we

have noted, lying in quite unsymmetrical environments. First we look in general at structures involving six-coordinated iron and four-coordinated arsenic and ask what the structural restrictions dictated by the composition of the material and the coordination numbers of the cations are. We can use them to probe compliance with Pauling's rules for structures such as these. The Pauling electrostatic bond strength associated with a leg of the iron octahedron is  $3/6$  and that for the arsenic tetrahedron is  $5/4$ . For an oxygen located at a vertex common to  $x$  octahedra and  $y$  tetrahedra, the electrostatic bond strength sum is just  $x(1/2) + y(5/4)$ . If Pauling's rule is satisfied, then this is equal to 2 so that and  $x$  and  $y$  are positive integral solutions of

$$2x + 5y = 8 \quad (3)$$

As  $2x$  and  $8$  are even,  $5y$  must be even too. Since  $5$  is odd,  $y$  must be even, and therefore the only possible solutions with positive integers are  $x = 4$ ,  $y = 0$ , there being no solutions with strictly positive integers. Thus we can immediately conclude from this simple argument that there is no structure containing linked iron octahedra and arsenic tetrahedra with the stoichiometry of angelellite where Pauling's rules is satisfied at all sites. The only solution contains isolated arsenic cations, uncoordinated ( $y = 0$ ) to oxygen. This result is a very simple one to derive, but of considerable importance. It tells us that purely on topological grounds, a "simple", "high-symmetry" structure for this material, given the cation coordination geometries, is not possible.

Arsenic however, is sometimes found in a five-coordinate environment, usually as a trigonal bipyramid. We can use the same approach to study this case, that of an angelellite stoichiometry but containing octahedral iron and five-coordinate arsenic. The same arguments may be used as before (see Appendix) to show that in this case there are structures which in principle obey the rule. (Although topologically possible, whether they are geometrically feasible is another matter of course.) Perhaps such a structure could be a high-pressure variant.

Thus the main conclusion of this section is that purely on topological grounds, a "simple", "high-symmetry" structure for this material, given the cation coordination geometries, is not possible. Similar considerations will be behind the structures of other "complex" materials too, especially those of minerals. However, as we will show later, although the *local* geometry is forced to be of low symmetry, a periodic repeating array is still electronically favored.

### Brown's and Pauling's Rules in an Orbital Context

The electrostatic bond strength ideas derived during the 1920s and 1930s, and still in use today in the mineralogical community, have been extended in recent years in a more general way to study the factors which control bond lengths and structures of a broader range of solids. In modern usage the electrostatic bond strength is replaced by the bond valence,<sup>13,14</sup> which is defined as

$$s = \exp((r - r_0)/B) \quad (4)$$

or alternatively as

$$s = (r/r_0)^{-N} \quad (5)$$

The parameter  $r_0$  is a reference bond length specific to a given pair of atoms as are the parameters  $B$  and  $N$ . The first definition is the more general of the two since there appears to be a universal value of  $B = 0.37$ . Often the reference bond length ( $r_0$ ) is allowed to depend upon formal oxidation state. Brown has extended Pauling's original ideas as two rules,<sup>13,14</sup> very useful in understanding how solids are assembled. The first Brown rule is effectively Pauling's second, but with the newer definition of  $s$ . At each atom  $\sum s = v$ , the valency of the atom. The parameters

(9) Pauling, L. *J. Am. Chem. Soc.* **1929**, *51*, 1010.

(10) Ellison, A. J. G.; Navrotsky, A. *J. Solid State Chem.* **1991**, *94*, 24.

(11) Burdett, J. K. *Prog. Solid State Chem.* **1984**, *15*, 173.

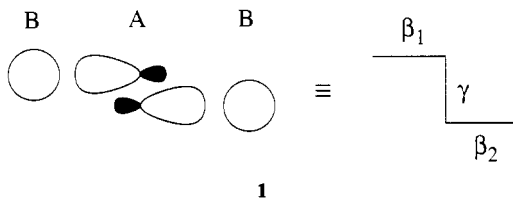
(12) Wheeler, R. A.; Whangbo, M.-H.; Hughbanks, T.; Hoffmann, R.; Burdett, J. K.; Albright, T. A. *J. Am. Chem. Soc.* **1986**, *108*, 2222.

(13) Brown, I. D.; Altermatt, D. *Acta Crystallogr.* **1992**, *B41*, 244.

(14) Brown, I. D. *Acta Crystallogr.* **1992**, *B48*, 553.

$r_0$  and  $N$ , obtained from a large structural database, are chosen to fit this equation. This is how  $v$  is (arbitrarily) introduced. (Elsewhere we show<sup>15</sup> the origin of this rule in an orbital context.) The systems for which these considerations apply are, by and large, insulators and certainly exclude systems such as metal alloys for which the structure is determined by Fermi surface effects controlled by electron count.<sup>16</sup> However, Brown's second rule leads to significant constraints on the possible structures. The rule states that for the same class of systems for which the first rule is applicable, at each atom the values of  $s$  for each of the  $\Gamma_i$  linkages around an atom are as equal as possible. The rule is particularly interesting since it is a statement which allows us to directly construct, if possible, a "high symmetry" structure where the bond lengths are equal. We show how such a rule comes from quite simple orbital arguments.

It will be convenient to use the bond orbital model<sup>17</sup> where the orbital picture is derived using pre-constructed  $sp$  hybrid orbitals on a central atom. Consider a simple orbital picture for an  $AB_2$  system where the central A atom is coordinated (1) to two B



atoms via two A–B linkages. The atom A carries two hybrids which point in the two directions. Figure 2 shows the construction of the molecular orbital diagram for such a system. Two values of  $\beta$  are used (1), one for the on-site interaction between the hybrids (we call this  $\gamma$ ) and one which links a hybrid orbital with a single orbital located on one of the ligands  $\beta_1, \beta_2$  ( $=\beta$  in the symmetrical structure). This orbital picture might represent an oxide where both of the deeper-lying (largely oxide) orbitals are filled with electrons. The resulting bonding orbitals, c are just the in-phase and out-of-phase combinations, b, of the hybrid orbitals, a (which regenerate  $s$  and  $p$  orbitals on the central atom respectively), with the corresponding combinations, d, of the B orbitals. The larger stabilization is afforded the symmetric combination since, from perturbation theory, the energy separation between the symmetrical hybrid combination and the B atom orbitals is smaller than for the antisymmetric one. (Recall that the energy of interaction of a pair of orbitals varies as the inverse of their energy separation.) Also shown in Figure 2 are the relative orbital coefficients of the bonding orbitals, exaggerated for effect. Both of these results are readily accessible from Hückel theory and this picture can be generated for a wide range of  $\gamma, \beta$ , and the parameter  $\Delta\alpha$ , which measures the energy separation between the orbitals in a and d. The next step is to see how the energy levels change on making the linkage asymmetric. First, a constraint is necessary to set the relative variation of  $\beta_1$  and  $\beta_2$  on distortion. Changes in interatomic distances found when structures are distorted, or when the coordination number changes, are often well-described electronically by a model with the constraint that the second moment of the energy density of states is held constant.<sup>16–19</sup> The second moment is simply given by the expression  $\sum_{i,j} H_{ij}^2$  over all of the linkages between the atom pairs  $i, j$  in the structure and is clearly a measure of coordination

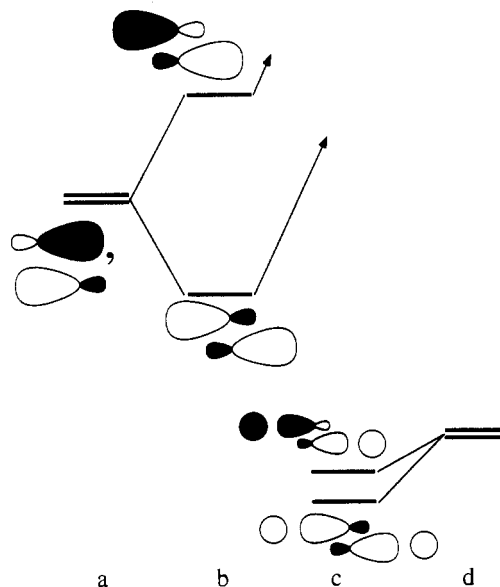
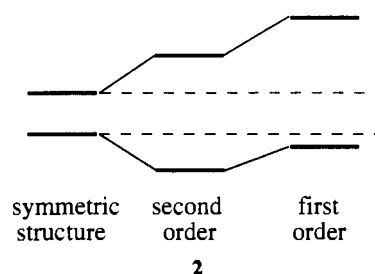


**Figure 2.** Construction of the molecular orbital diagram for the four-orbital system appropriate for an  $AB_2$  molecule where the central A atom is coordinated to two B atoms via two A–B linkages. The difference in electronegativity of the two atoms is represented by different values of  $\alpha$  for the hybrid orbitals on A and the single orbitals included at each B center. Key: (a) the two non-interacting hybrids, (b) the in- and out-of-phase combinations of the two, separated in energy by  $2\gamma$ ; (c) the result of interaction with the B orbitals (d).

strength. Using this constraint implies that in the construction of the modified energy level diagram the sum  $(\beta_1^2 + \beta_2^2)$  should be kept constant. How the bonding orbitals of Figure 2c change in energy on distortion (2) may be viewed simply using perturbation



theory. The second-order shifts will on the simplest scheme depress the lower, symmetric combinations and elevate the upper, antisymmetric combinations equally. However the first order changes will be different. They are proportional to the function  $c_1 c_2 (\Delta\beta_1 + \Delta\beta_2)$  where  $c_1$  and  $c_2$  are the hybrid and ligand coefficients of the two bonding orbitals. (Using the fact that the sum  $\beta_1^2 + \beta_2^2 = 2\beta^2$ ,  $(\Delta\beta_1 + \Delta\beta_2) = -[(\Delta\beta_1)^2 + (\Delta\beta_2)^2]/2\beta > 0$ . (The energy changes in 2 are exaggerated for effect; the second-order change is numerically smaller than the first from sample calculations.) Thus, the two bonding orbitals are destabilized in first order on making the linkages asymmetric. Since  $c_1 c_2$  is larger for the symmetric combination (clear from Figure 1c), the overall result is that the antisymmetric combination is destabilized more than the symmetric combination is stabilized. An important consequence of this result is that for two pairs of electrons the symmetric structure is stabilized relative to the asymmetric one, but the converse is true for just one pair. The stabilization energy for the most common case, where these two bonding orbitals are both occupied, is thus maximized for the case where the two bonds are of the same strength (length) and  $\beta_1^2 = \beta_2^2$ . Here therefore is the electronic basis behind Brown's second rule.

Figure 3b shows the application of the same philosophy to the  $\sigma$  system of cyclic molecules of the type  $A_2B_2$  where both A and

- (15) Burdett, J. K.; Hawthorne, F. C. *Am. Mineral.* **1993**, *78*, 884.  
 (16) Hoistad, L. M.; Lee, S. *J. Am. Chem. Soc.* **1991**, *113*, 8216. Hoistad, L. M.; Lee, S.; Pasternak, J. *J. Am. Chem. Soc.* **1992**, *114*, 4790. Lee, S. *Acc. Chem. Res.* **1991**, *24*, 249. Lee, S. *J. Am. Chem. Soc.* **1991**, *113*, 101. Lee, S. *J. Am. Chem. Soc.* **1991**, *113*, 8611.  
 (17) Harrison, W. A. *Electronic Structure and The Properties of Solids*; Freeman: San Francisco, CA, 1980. Levin, A. A. *Solid State Quantum Chemistry*; McGraw-Hill: New York, 1977.  
 (18) Pettifor, D. G.; Podloucky, R. *J. Phys.* **1986**, *C19*, 285.  
 (19) Burdett, J. K.; Lee, S. *J. Am. Chem. Soc.* **1985**, *107*, 3063.

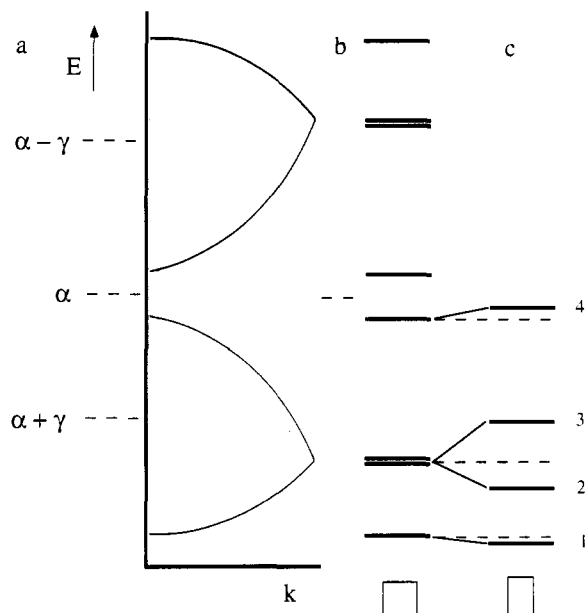
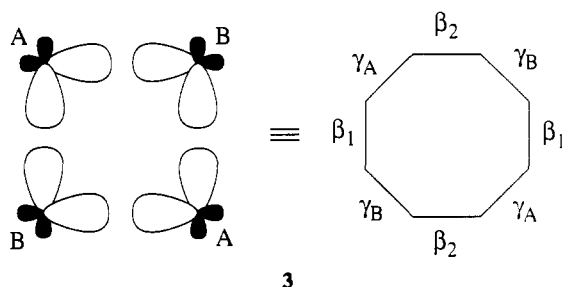


**Figure 3.** (a) Energy levels of a one-dimensional chain with a unit cell stoichiometry of AA, isomorphous with the levels of the square  $A_4$  molecule (b). Shown in part c in an exaggerated way is how the lowest four levels change during a distortion which makes adjacent distances unequal.

B atoms carry a pair of hybrid orbitals (3), or the parent

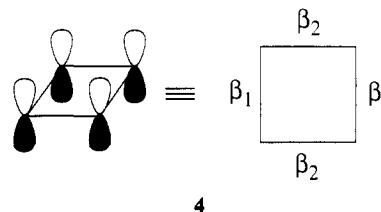


homoatomic  $A_4$  molecule itself. The calculations are those appropriate for the latter. This system is isomorphous<sup>11</sup> (Figure 3a) with the orbital patterns at the zone center and edge of a one-dimensional chain of stoichiometry AB or the parent AA chain. Figure 3c shows the way the four lowest energy levels change during a distortion which makes adjacent linkages inequivalent. The interpretation of the energy changes is in fact similar to that found in 2. As a pair, orbitals 1 and 4 are destabilized on distortion, as are likewise 2 and 3. Thus, important for the case of four bonding pairs in these lowest four orbitals, the square is stable with respect to the distortion, which makes the two AA distances inequivalent. A very similar picture is found for the case where the  $\alpha$  values of the two sets of hybrids are different, namely the situation for the  $A_2B_2$  molecule. For the infinite solid, assuming that the sum of the energies at the zone edge and center is a good way to average the energy across the Brillouin zone, the lowest energy structure is the periodic structure with equal nearest-neighbor distances. This result is good evidence for the stability of the infinite crystal with equal bond lengths, although we clearly have not derived the energy of some aperiodic structure to test the result further.

The opposite result comes from the bare ionic model. If  $E_{ij} \propto -1/r_{ij}$ , assuming  $\Delta r_{12} = -\Delta r_{13}$ ,  $E_{12} + E_{13} \propto -(1/(r + \Delta r) + 1/(r - \Delta r))$  an expression which is minimized for  $\Delta r \neq 0$ . The same result is true of any  $r^{-n}$  attractive model. The "correct" result comes from a model which includes both attractive and repulsive forces. If  $V = -A/r + B/r^n$ , then the total energy at equilibrium is  $E_{12} + E_{13} \propto -A/r_e(1 - (1/n))$ . On distortion as before by  $\pm\Delta r$ ,  $E_{12} + E_{13} \propto -A/r_e(1 - (1/n)) + nA(\Delta r/r_e)^2$ , a

function minimized for  $\Delta r = 0$ . A similar result comes from the assumption of harmonic forces between nearest-neighbor atoms. If  $E \propto (\Delta r)^2$ , then  $E_{12} + E_{13} \propto (r + \Delta r)^2 + (r - \Delta r)^2 = 2(\Delta r)^2$ , minimized for  $\Delta r = 0$ , i.e., where the two bonds are of the same length. The same result applies to a system where a repulsive potential exists of the form  $E \propto \exp(-r_{ij})/\rho$ . Then  $\Delta E \propto 2 \exp(-r/\rho) [\cosh(\Delta r/\rho)]$ , a function which is positive but minimizes as well for  $\Delta r = 0$ . In all of these models the analog of the constant second moment is the constant bond length sum.

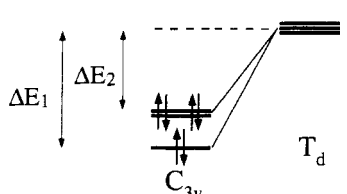
The opposite result comes too from a half-filled collection of orbitals of the same type. We know that the half-filled collection of  $p\pi$  orbitals in cyclobutadiene (4) leads to a first-order Jahn–



Teller distortion of the square, such that adjacent bonds alternate in length. In benzene there is a similar second-order Jahn–Teller stabilization of the alternating structure from the  $\pi$  manifold, but here the symmetric structure is found. Hiberty, Shaik, and co-workers<sup>20</sup> have shown that it is the energetic demands of the  $\sigma$  manifold (described above) that frustrate such a distortion and stabilize the regular structure. In push–pull cyclobutadienes, equal bond lengths are found. This arises simply as a result of the decrease in the second order distortion energy associated with the increase in the HOMO–LUMO gap of the substituted molecule relative to the parent. In other small molecules the sign of adjacent bond–bond interaction force constants are frequently accessible<sup>7</sup> using second-order Jahn–Teller arguments. Even when these are positive, indicating a softening of the antisymmetric stretching distortion, the equilibrium geometry of the molecule is a symmetric one. In solids, geometry changes as a result of Fermi surface instabilities associated with the highest occupied levels are similarly resisted by the stiffness of the underlying framework. Thus although polyacetylene undergoes a Peierls distortion to give alternating C–C distances, the analogous distortion in graphite is not found due to the rigidity of the  $\sigma$  skeleton.<sup>11</sup>

Orbital arguments may be used to view angular geometry changes. It is a simple matter to show electronically why the tetrahedral  $AB_4$  geometry is the lowest energy angular arrangement for a four-coordinated octet compound for either the "anion" or the "cation". Our theoretical considerations should in principle be applied to the band structure of the solid, but the essence of the arguments will be apparent from the consideration of the electronic structure of a local unit, which one can envisage as capturing the electronic picture at the Brillouin zone center. The orbital picture is somewhat simpler and is accessible using a  $p$ -orbital model. Consider an octet  $AH_4$  molecule from the standpoint of the Rundle–Pimentel model.<sup>7</sup> Here one electron pair is assumed to be stereochemically impotent and is placed in the central atom  $ns$  orbital and the geometry controlled by the energetics of the  $np$ -ligand  $\sigma$  manifold of orbitals. Figure 4 shows the energies of the three  $p$  orbitals within the framework of the angular overlap model<sup>7</sup> during a  $C_{3v}$  distortion. Notice that the summed second order energy is angle independent (via Unsöld's theorem), but the fourth-order term is minimized at the tetrahedral geometry ( $\cos \theta = 1/3$ ). Similar arguments<sup>15</sup> show how the octahedral geometry is the one predicted for the six-coordinate system. These are purely orbital arguments but ones which lead

(20) Shaik, S. S.; Hiberty, P. C. *J. Am. Chem. Soc.* **1985**, *107*, 3089. Ohanessian, G.; Hiberty, P. C.; Lefour, J.-M.; Flament, J.-P.; Shaik, S. S. *Inorg. Chem.* **1988**, *27*, 2219.

$$\begin{aligned}\Delta E_1 &= e_{\sigma}(1 + 3\cos^2\theta) - f_{\sigma}(1 + 3\cos^2\theta)^2 \\ \Delta E_2 &= (3/2)e_{\sigma}\sin^2\theta - f_{\sigma}(3/2)^2\sin^4\theta \\ \Delta E_{\text{Total}} &= 8e_{\sigma} - 2f_{\sigma}[(1 + 3\cos^2\theta)^2 + 2(3/2)^2\sin^4\theta]\end{aligned}$$


**Figure 4.** Energies of the three occupied molecular orbitals derived from the central atom *p* orbitals (the Rundle–Pimentel model) within the framework of the angular overlap model during a  $C_{3v}$  distortion.

to the same conclusions concerning the geometry as steric, Coulombic, and VSEPR arguments. Minimization of this fourth-order term and its analog in the  $AB_6$  fragment leads to the result that the most “symmetric” structure is the one which is most stable for the electronic configuration where half of the relevant orbitals of the problem are filled with electrons. Thus regular tetrahedra and octahedra are the local geometries expected on electronic grounds. The result obtained from Figure 4 may be viewed within the framework of the Schwartz inequality. The fourth-order term will be minimized when the second-order contributions are as equal as possible. We have used<sup>6</sup> the term “metriotic” to describe this state of affairs. For the half-filled electronic situation where all of the bonding orbitals are occupied, then the most stable geometry is not the one where some orbitals are overutilized compared to others but the geometry where the orbital interactions are as equal as possible. Although this was not shown algebraically for the case of the  $AB_2$  molecule, the  $A_2B_2$  square, or the  $AB$  infinite solid, Brown’s second rule is just one facet of this much broader result. Away from this rather special electronic situation these rules do not hold. There is now no requirement for the most “symmetric” environment to be the most stable. The discussion associated with Figure 4 requires summation of the stabilization energy of all the bonding orbitals. The same result will not hold if only some of these deep-lying orbitals are occupied or if some of the higher energy ones are occupied. Indeed  $SF_4$  in contrast to  $CF_4$  is not tetrahedral; in contrast to  $NaCl$  where each linkage is identical, in  $ZrCl$  there are linkages of two different types around each  $Zr$  atom ( $Zr-Cl$  and  $Zr-Zr$ ).

It is worthwhile to briefly summarize at this point in the paper. Some compositions, because of stoichiometry and connectivity may lead to “symmetrical” structures (e.g.,  $NaCl$ ). Others (such as angelellite) may not. Systems where all of the relevant bonding orbitals are filled and antibonding ones empty (the half-filled electronic situation as described in the next section), such as in most mineral structures, the octets etc., are associated with an electronic driving force ensuring the equivalence of bonds around each center where possible given the topological restrictions described above. This is in the absence of first- or second-order Peierls distortions. For the simple high-symmetry cases (e.g.,  $NaCl$ ), this leads to the generation of a crystal with its equal bond lengths propagated through the crystal via the picture of Figure 3. For lower symmetry systems, forced to be so by the stoichiometry and connectivity (e.g., angelellite) or by Fermi surface instabilities, it is not clear that such a crystal will be generated from the local structure. For systems with other electron counts, no prediction is made as to the stability of the regularly repeating extended array.

### The Coloring Problem

An important aspect of the structures of solids which adopt a derivative structure of some type, is how the atoms are ordered

over the sites of the parent. We have called<sup>21</sup> this the “coloring problem” since we ask the traditional combinatorial question of how many different ways there are to color the sites of a parent structure, the number of colors being set by the number of different atoms involved. Some of the patterns may be ordered ones, leading to a crystalline material; some may be disordered. How the atoms are ordered clearly leads to either highly “symmetric” or not so “symmetric” structures. Here we are particularly interested in the energetics involved in the coloring of first, second, etc., neighbor sites. In rock salt, sphalerite, cadmium halide, and indeed in most octet solids, the first nearest neighbors are of the opposite type (i.e.,  $Na$  is surrounded by six  $Cl$  atoms in rock salt), the second are of the same type (i.e.,  $Na$  is surrounded by 12  $Na$  atoms in rock salt). The traditional viewpoint has for many years been that derived from the ionic model. Clearly if the solid is composed of positively and negatively charged billiard balls, then the lowest energy arrangement will be the one where close contacts between positive and negative charges are encouraged and contacts between ions of like charge discouraged. The focus of the present paper is however on electronic mechanisms. There is a very useful way to study this question from an electronic point of view which uses two ideas from the method of moments.<sup>6</sup>

The first powerful result is that the energy difference curves between two structural alternatives as a function of electron count,  $\Delta E(x)$ , very often have a well-defined shape. We define the parameter  $x$  as a fractional orbital occupancy or band filling in the following way: empty,  $0 < x < 1$ , full. The curve representing the energetic difference between two systems whose densities of states differ at the  $n$ th moment frequently have  $n$  nodes (including the two at  $x = 0, 1$ ) as shown in Figure 5 for  $n = 2-6$ . The structure with the largest moment is the one stable at the earliest band fillings, thus defining the sign of  $\Delta E$  for a given problem. This provides a very useful way to look at structural problems. Whereas one might be interested in the value of  $\Delta E$  for a single system with a given electron count, generation and analysis of the entire  $\Delta E(x)$  curve provides a much broader picture of the structural problem.

The second result is the connection between the moments themselves and the geometrical structure. The  $n$ th moment of the energy density of states may simply be expressed in terms of  $H$ , the Hamiltonian matrix and its individual elements,  $H_{jk}$

$$\begin{aligned}\mu_n &= \text{Tr}(H)^n \\ &= \sum_j \sum H_{jk} H_{kl} \dots H_{zj}\end{aligned}\quad (6)$$

The second sum in eq 6 runs over all products of order  $n$ . This means that the  $n$ th moment is simply the weighted sum of all the walks of length  $n$  which start off on orbital  $j$  and return to that orbital in  $n$  steps (Figure 6a). The weights are simply the interaction or hopping integrals  $(H_{lm})$  between the two orbitals  $l$  and  $m$  involved in the step, and is usually set proportional to the relevant overlap integral, namely  $S_{lm}$ . Note that walks in place are included with weights  $H_{mm}$ . The powerful theoretical tool which comes from such an approach is that evaluation of the walks that are *different* between the structures to be compared immediately defines the expected shape of the energy difference curve. Notice that the amplitude of the curves in Figure 5 decrease with increasing  $n$ . This result is simple to understand in terms of this topological connection. Energetic differences controlled by first nearest-neighbor interactions (and therefore involving a walk of length 2, Figure 6b) will be larger than those controlled by second nearest neighbors (and therefore involving a walk of length 4) which in turn will be larger than those controlled by third nearest neighbors (and therefore involving a walk of length 6).

(21) Burdett, J. K.; McLarnan, T. J.; Lee, S. *J. Am. Chem. Soc.* **1985**, *107*, 3083.

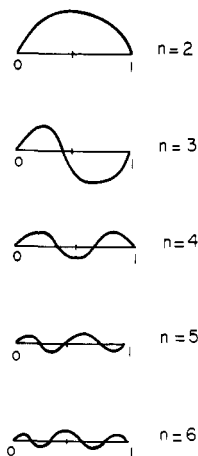


**Figure 5.**  $\Delta E(x)$  curves which representing the energetic difference between two systems whose densities of states differ at the  $n$ th moment. The parameter  $x$  is the fractional orbital occupancy or band filling and is defined as follows: empty,  $0 < x < 1$ , full.

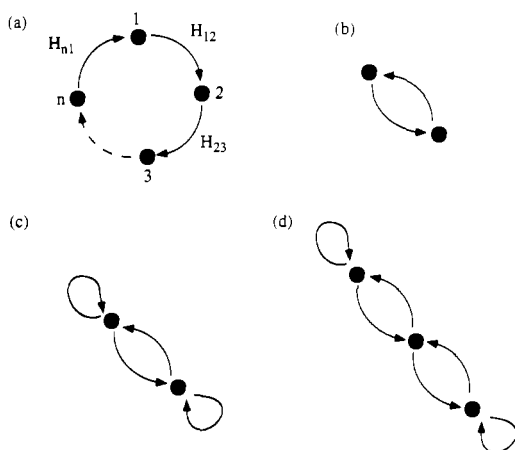


**Figure 6.** (a)  $n$ th moment in terms of the self-returning walks through the structure. (b) Second moment, via a walk of length 2, as a measure of first nearest-neighbor interactions. (c) Choice of first nearest-neighbor as a result of a walk of length 4. (d) Choice of second nearest-neighbor as a result of a walk of length 6.

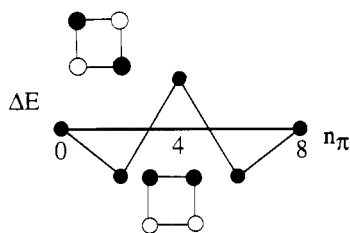


**Figure 7.** Calculated  $\Delta E(x)$  plot for the cis and trans isomers of substituted cyclobutadienes using simple Hückel theory.

Although we have described the energetics determining the first nearest-neighbor interactions as a second moment one, as Figure 6c shows, the *choice* of first nearest neighbor is a fourth moment problem. This is clear to see since it takes a walk of length 4 for an atom to interrogate its first nearest neighbor and decide whether it is chemically different (i.e., has a different  $\alpha$  value). A calculated  $\Delta E(x)$  plot<sup>6</sup> for the cis and trans isomers of substituted cyclobutadienes using simple Hückel theory is shown in Figure 7. Square cyclobutadienes are best stabilized by attaching electron-donating and -withdrawing groups alternately around the ring, found in the so-called push-pull cyclobutadienes. The plot is thus in agreement with experiment. (Stabilization of this pattern is also found in the solid-state structure of  $\text{CaB}_2\text{C}_2$ .) Notice that the number of nodes indicates that this is indeed a fourth moment problem. In reading such energy difference curves

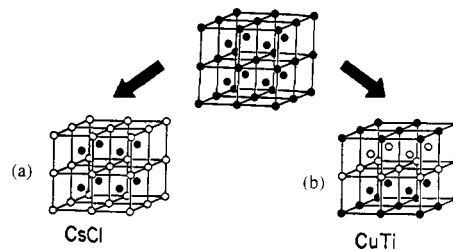


**Figure 8.** Two of the simplest two-color patterns of the bcc structure: (a) the CsCl and (b) the CuTi arrangements.

**Table 1.** Moments of Two Model Structures, the Infinite Chains (...ABAB... and ...AABB...)

...ABAB...	
(a) All $\beta$ Equal	$\mu_1 = 2(\alpha_A + \alpha_B)$
	$\mu_2 = 2(\alpha_A^2 + \alpha_B^2 + 4\beta^2)$
	$\mu_3 = 2(\alpha_A^3 + \alpha_B^3 + 6\beta^2(\alpha_A + \alpha_B))$
	$\mu_4 = 2(\alpha_A^4 + \alpha_B^4 + 12\beta^2(\alpha_A^2 + \alpha_B^2 + 8\alpha_A\alpha_B\beta^2))$
(a) Unequal $\beta$	$\mu_1 = 2(\alpha_A + \alpha_B)$
	$\mu_2 = 2(\alpha_A^2 + \alpha_B^2 + 4\beta_{AB}^2)$
	$\mu_3 = 2(\alpha_A^3 + \alpha_B^3 + 6\beta_{AB}^2(\alpha_A + \alpha_B))$
...AABB...	
(c) All $\beta$ Equal	$\mu_1 = 2(\alpha_A + \alpha_B)$
	$\mu_2 = 2(\alpha_A^2 + \alpha_B^2 + 4\beta^2)$
	$\mu_3 = 2(\alpha_A^3 + \alpha_B^3 + 6\beta^2(\alpha_A + \alpha_B))$
	$\mu_4 = 2(\alpha_A^4 + \alpha_B^4 + 12\beta^2 + 10\beta^2(\alpha_A^2 + \alpha_B^2) + 4\alpha_A\alpha_B\beta^2)$
(d) Unequal $\beta$	$\mu_1 = 2(\alpha_A + \alpha_B)$
	$\mu_2 = 2(\alpha_A^2 + \alpha_B^2 + 2\beta_{AB}^2 + \beta_{AA}^2 + \beta_{BB}^2)$
	$\mu_3 = 2(\alpha_A^3 + \alpha_B^3 + 3\beta_{AB}^2(\alpha_A + \alpha_B) + 3(\alpha_A\beta_{AA}^2 + \alpha_B\beta_{BB}^2))$

it is always the arrangement with the larger  $n$ th moment which is the one which is most stable at the earliest electron counts. This means that for the fourth moment problem it is the arrangement with the smaller fourth moment (the ...ABAB... pattern) which is most stable at the half-filled point. A little counting allows confirmation of the fourth moment nature of the structural problem controlled by the structure of the nearest neighbor contacts. Table 1 shows the moments of two model structures, the infinite chains (...ABAB... and ...AABB...). If values of the hopping integrals are kept equal for all contacts, irrespective of their nature, assuming two different  $\alpha$  values, but setting  $\beta_{AA} = \beta_{BB} = \beta_{AB} \equiv \beta$ , then the only differences between the two arrangements arise as a result of the walks in place. From Table 1 it is clear that the first disparate moment is the fourth, and thus four nodes are expected in  $\Delta E(x)$  as observed. It is the structure with the smaller fourth moment which should be observed at half-filling, namely the "symmetrical" structure ...ABAB...

Similar pictures apply to solid-state problems in general. For example a  $\Delta E(x)$  curve (from a band structure calculation) between the two simplest two-color patterns of the bcc structure for the case of transition metal alloys is very similar<sup>21</sup> to that of Figure 7. The structures under consideration are the CsCl and CuTi arrangements of Figure 8. Here too the structure which is calculated (and found) to be most stable at the half-filled point (CsCl) is the one containing A-B contacts, whereas the structure stable in the other two regions is the one where there are both A-A and B-B contacts. Of note too is that the CsCl structure is the high-symmetry (cubic,  $Z = 1$ ) structure, but the CuTi structure is of lower symmetry (tetragonal) and is more "complex" ( $Z = 2$ ).

Exactly analogous ideas apply to systems with  $\text{AB}_n$  stoichiometry. Electron counting however, is important here. For an  $\text{AB}_2$  structure for example (e.g.  $\text{ZnCl}_2$ ) the B atom orbitals are filled for 16 electrons. Of these, only eight lie in the four bonding, B-located orbitals (which complement the four antibonding orbitals located on the A atom). The other eight lie in four

nonbonding, B-located orbitals. Thus as far as the value of  $x$ , the fractional orbital occupancy, is concerned, these systems correspond to half-filled band arrangements; i.e., half of the orbitals involved in bonding or antibonding interactions are filled. Partial occupancy of the metal d orbitals usually leads to relatively small changes in the general structural picture. Thus first-order Jahn–Teller distortions of the basic cadmium halide or rutile structure are found for salts of Cu(II), with second-order Jahn–Teller distortions of this structure found for salts of Hg(II), and trigonal prismatic geometries are frequently found for early transition metal dichalcogenides. On structure maps these distorted variants lie<sup>22</sup> within the field of their parent, suggesting that the major features of the structure are determined by cation s, p orbital interactions with the anions. This is a viewpoint supported by the form of the structure map<sup>23</sup> which distinguishes between normal and inverse spinels. The traditional CFSE arguments only appear to be important in distinguishing one from the other at the boundary between the two structures set by the “s + p” forces. Sometimes, even when the local distortion is large, the general features of the structure are preserved. Thus PdS<sub>2</sub>, which contains a square planar Pd atom, is still based on the pyrite structure. There will be some exceptions to this point of view below.

The walks (Figure 6d) which distinguish second nearest neighbors in the structure clearly show that it is the sixth moment which controls the energetics here. Figure 4 shows a sixth moment plot. Notice now that because of the number of nodes, at the half-filled point the structure is stabilized by the presence of like second-nearest neighbors. Analogous arguments clearly show how this is extended to neighbors further way. The identity of the stable  $n$ th neighbor alternates between like and unlike neighbors simply because of the identity of the stable structure at the half-filled point in the  $2(n + 1)$ th moment plot.

From the discussion above a general, very powerful, result emerges concerning the structures of binary and more complex compounds. At the point where the collection of energy levels is half-filled (and we include systems with partially filled d levels here too; vide supra) the most stable structural alternative of all of the coloring patterns, is predicted to be the structure where odd nearest-neighbor heteroatomic contacts and even nearest-neighbor homoatomic contacts are maximized. This leads to a certain symmetry for the most stable structure. For this reason, octet compounds tend to adopt those structures where the electronegativities of the atoms alternate. Sphalerite (zincblende) (ZnS) contains alternating zinc and sulfur atoms, just as in the more complex diamond derivative structures such as chalcopyrite, stannite and nowackiite. All of the classic octet structures are of this type (CsCl, NaCl, ZnS, ZnO, CdHal<sub>2</sub>, CaF<sub>2</sub>, TiO<sub>2</sub>, etc.). In all of these solids with four electrons per atom, the bonding orbitals are completely occupied and all of the antibonding ones unoccupied. The fractional orbital occupation is thus 0.5. Away from the half-filled point, the identity of the stable coloring patterns now change. Depending on the system, the structural preferences for the  $n$ th nearest neighbor will change. Thus many structural possibilities will now exist. As noted already, the simplest ...AABB... structure is in general of lower symmetry than ...ABAB.... Thus, as is apparent from Figure 8, the CsCl arrangement is cubic but the CuTi structure is tetragonal.

There are several examples of such ...AABB... structures. For example, the structure of GaSe is derived from that of wurtzite and has a stacking structure ...GaGaSe.... The structures of ZrCl and ZrBr are interesting ones in that they contain a ...ZrZrXX... pattern. This case is readily understood in terms of the metal–metal bonding between adjacent zirconium sheets made possible by the d<sup>3</sup> electron configuration for Zr(I). Both examples are

ones where there are extra electrons relative to the half-filled situation. (The ZrCl example is one where the s + p model for transition metal systems described earlier fails. The metal d orbitals are crucial here.)

### Coloring Of Bonds

Analogous results apply to the coloring of bonds, and as we will see, the approach leads to the development of a broad electronic picture. It is a simple matter to count the walks and evaluate the moments of the initially square system for the  $\sigma$  (3) and  $\pi$  (4) manifolds. The two are radically different. The odd moments are zero for both systems, and as we have described elsewhere<sup>6</sup> the contribution to the fourth moment from walks originating from each orbital in the  $\pi$  case (4) is given by  $\beta_1^4 + \beta_2^4 + 6\beta_1^2\beta_2^2 = (\beta_1^2 + \beta_2^2)^2 + 4\beta_1^2\beta_2^2$ . Using the constant second moment constraint, this is largest for the case where  $\beta_1 = \beta_2$ , and thus at half-filling the distorted structure should be found. These are just the first- and second-order Jahn–Teller predictions for the homo- (A<sub>4</sub>) and heteroatomic (A<sub>2</sub>B<sub>2</sub>) systems respectively. Such results are applicable to the one-dimensional chain too since the levels of the square are just those at the zone center and edge of the infinite structure and here leads to the Peierls distortion. For the  $\sigma$  manifold the moments are readily evaluated from 3. For simplicity we treat the homoatomic case with  $\gamma_A = \gamma_B = \gamma$ . The contribution to the fourth moment from walks originating a pair of adjacent orbitals is  $\beta_1^4 + \gamma^4 + 2\beta_1^2\gamma^2 + \beta_1^2\gamma^2 + \beta_2^2\gamma^2$  and  $\beta_2^4 + \gamma^4 + 2\beta_2^2\gamma^2 + \beta_2^2\gamma^2 + \beta_1^2\gamma^2$ , which when summed give  $(\beta_1^2 + \beta_2^2)^2 - 2\beta_1^2\beta_2^2 + 2\gamma^4 + 4\gamma^2(\beta_1^2 + \beta_2^2)$ . In contrast to the  $\pi$  case the largest fourth moment is now found for the distorted case where  $\beta_1 \neq \beta_2$ , which means that at the half-filled point the symmetric structure should be found. This is a somewhat more satisfying proof than that from Figures 2 and 3 of local bond length equality. The spirit of the moments method views structural preferences as a function of electron count, and from the form of the fourth moment curve of Figure 5, the distorted structure should be stable for earlier electron counts. This result was in fact described earlier using the result from Figure 2. The relevance of the result for the half-filled band to the topic of this paper is obvious. There is an electronic stabilization of the state of affairs where adjacent bonds are equal in length. Thus, where topologically possible, all nearest neighbor distances are equal.

### Moments, Disorder, and Crystals

One of the concerns of an earlier section went beyond arguments concerning the local geometry to the idea of the crystal. It is interesting to explore how the long-range order/disorder problem can be viewed within the moments language. Recall that the disordered system, since it lacks translational periodicity, is not susceptible to a simple electronic description based on the traditional Bloch picture. However, the moments approach will be a perfectly satisfactory one since there is no such restriction of this type. Consider the chain of stoichiometry AB in which each site is statistically occupied by half A and half B atoms. The two simplest ordering patterns are those described earlier, namely ...ABAB... and ...AABB.... The moments may be computed in a completely general way by the introduction of an order parameter in the mean-field sense. The simplest form possible for this is to write  $P_i(A) = 1/2(1 + \psi_0)$  as the probability of finding an A atom on any given site  $i$ . When  $\psi_0$  is zero the system is completely disordered with an equal probability of finding A or B at either site. When  $\psi_0$  is equal to 1 then the system is completely ordered and either the ...ABAB... or ...AABB... structure is found. Tables 2 and 3 show the site occupancy probabilities. Recalling that the first disparate moment between two structures dictates the energy preference as a function of band filling, the function  $\Delta\mu^i(\psi_0) = \mu^i(\psi_0) - \mu^i(0)$  measures the difference between a partially ordered ( $0 < \psi_0 < 1$ ) or ordered ( $\psi_0 = 1$ ) systems and the fully disordered ( $\psi_0 = 0$ ) chain. Since the stoichiometry of the chain is AB,

(22) Burdett, J. K. *J. Met. Alloys* **1993**, *197*, 281.

(23) Burdett, J. K.; Price, S. L.; Price, G. D. *J. Am. Chem. Soc.* **1982**, *104*, 92.



**Table 2.** Site Probabilities for ...ABAB... Chains

site ...ABAB...	atomic species	
	A	B
<i>i</i>	$1/2(1 + \psi_0)$	$1/2(1 - \psi_0)$
<i>j</i>	$1/2(1 - \psi_0)$	$1/2(1 + \psi_0)$

**Table 3.** Site Probabilities for ...AABB... Chains

site ...AABB...	atomic species	
	A	B
<i>i</i>	$1/2(1 + \psi_0)$	$1/2(1 - \psi_0)$
<i>j</i>	$1/2(1 + \psi_0)$	$1/2(1 - \psi_0)$
<i>k</i>	$1/2(1 - \psi_0)$	$1/2(1 + \psi_0)$
<i>l</i>	$1/2(1 - \psi_0)$	$1/2(1 + \psi_0)$

**Table 4.** Moments of ...AABB... Chain as a Function of Order Parameter

<i>i</i>	$\mu^i(\psi_0)$
1	$\alpha_A + \alpha_B$
2	$\alpha_A^2 + \alpha_B^2 + (1 - \psi_0^2)(\beta_{AA}^2 + \beta_{BB}^2) + 2(1 + \psi_0^2)\beta_{AB}^2$
3	$\alpha_A^3 + \alpha_B^3 + 3(1 - \psi_0^2)(\alpha_A\beta_{AA}^2 + \alpha_B\beta_{BB}^2) + 3\beta_{AB}^2(1 + \psi_0^2)(\alpha_A + \alpha_B)$
4	$\alpha_A^4 + \alpha_B^4 + 3(1 - \psi_0^2)(\beta_{AA}^4 + \beta_{BB}^4) + 6(1 - \psi_0^2)(\alpha_A^2\beta_{AA}^2 + \alpha_B^2\beta_{BB}^2) + 6\beta_{AB}^4(1 + \psi_0^2) + 4\beta_{AB}^2(1 + \psi_0^2)(\alpha_A^2 + \alpha_B^2 + \alpha_A\alpha_B)$

independent of order, we know that  $\Delta\mu^1 \equiv 0$ . Table 4 shows the values of the first four moments (normalized to two sites) for the ...ABAB... chain and Table 5 those for the ...AABB... chain. As in the *n*th nearest-neighbor problem above, the situation may be simplified to just an electronegativity perturbation, assuming two different  $\alpha$  values, but setting  $\beta_{AA} = \beta_{BB} = \beta_{AB} \equiv \beta$ . Simple substitution shows that  $\Delta\mu^i = 0$  for  $i = 1-3$ , but  $= \pm\beta^2\psi_0^2\Delta\alpha^2$  ( $\Delta\alpha = \alpha_1 - \alpha_2$ ) for  $i = 4$ . (The positive sign is found for ...ABAB... and a negative sign for ...AABB....) Thus, not unexpectedly, the first disparate moment is the fourth, just as in the cyclobutadiene coloring problem, where the system with the smaller fourth moment is favored at the half-filled band. Figure 9 shows the plot of  $\Delta\mu^i(\psi_0)$ ,  $i = 4$ . The fourth moment becomes smaller (more negative) with increasing order until the minimum is reached at the fully ordered  $\psi_0 = 1$  ...ABAB... structure. The analogous result for the ...AABB... structure is that the fourth moment increases with  $\psi_0$ . So the disordered structure always has a fourth moment located between the two ordered patterns. Thus on this nearest-neighbor model, for an electron count where the most stable structure is the one with the smaller fourth moment, then the ordered ...ABAB... structure is predicted to be most stable, and for an electron count where the most stable structure is the one with the larger fourth moment, then the ordered ...AABB... structure is predicted to be most stable. For no electron count is the disordered structure stable.

Exactly analogous arguments may be used for the related problem where the bonds are colored rather than the atoms. Now there are the possibilities ...abab... and ...aabb..., in place of ...ABAB... and ...AABB.... For the simplest case, that of 3,  $\Delta\mu^4 = 4(\beta_1^2 - \beta_2^2)^2$  for the two ordered extremes, where the  $\alpha$  values are the same for all atoms but there are two different  $\beta$  values,  $\beta_a$  and  $\beta_b$ . The ...abab... structure has the smaller fourth moment. Thus at the half-filled point the theory leads to the result that the ordered, crystalline structure ...abababababab... is more stable than any other variant. So the system may be susceptible to a Peierls distortion or other Fermi surface instability, but the distortion pattern is a regular one extended indefinitely. An analogous picture holds for the case in 4, except that here it is a sixth moment problem. At the half-filled point, it is the ...abab... array, which is more stable. This may be a simple one-dimensional model for angelellite where the labels a and b represent bonds of different length, forced to be so by local geometry considerations. Results analogous to those obtained for the stability of the next-nearest atomic neighbors above apply to this case too in terms of the stable structures for the bonds. The complete set of results thus indicate stability for this arrangement for all

moments at the half-filled point and thus stability of the infinite crystalline material. Away from the half-filled point, other possibilities arise. A particularly interesting electronic situation is that where the electron count is such that it falls on a node of the energy difference curve. Either the result may be a more complex structure with features of both possibilities (actually found for the structure of AuSn<sub>2</sub><sup>24</sup>) or it is possible that a disordered system exists at finite temperatures, the energy differences between a variety of structural possibilities being rather small.

### A Broader Perspective

Many traditional arguments concerning the stability of particular arrangements in solids center around electrostatic considerations. Clearly the alternating arrangements of electropositive and electronegative atoms (ions) found in many octet solids are consistent with this view. However, electrostatic arguments should apply irrespective of whether the system is an octet or not. The different type of structure frequently found for the nonoctets is surely indicative of the importance of other types of interactions. The orbital model used here treats systems equally irrespective of electron count, and the different structural features found away from half-filling are understandable in principle using this broader approach. The powerful moments approach is a smooth way to link the electronic structures of crystalline and noncrystalline materials.

We have been able to demonstrate the following for one-dimensional orbital problems: (a) For the half-filled electronic situation in sp-bonded networks, (i) the lowest energy structure is one where "anion" and "cation" alternate, (ii) if a symmetric local structure is possible on topological-stoichiometric grounds, then it will be (Brown's second rule), and (iii) the local structure, symmetric or not, will translate to a periodic array. (b) For the half-filled band of orbitals of one type susceptible to Fermi surface instabilities, (i) although the local structure may not be symmetric as a result, a translationally periodic structure is of lowest energy, and (ii) electronegative and electropositive atoms alternate in the structure. (c) For electronic situations away from the half-filled point, a translationally repeating structure is predicted, but the identity of first, second, etc., nearest neighbors depends on the electronic details.

**Acknowledgment.** This research was supported by The Office of Naval Research and by NSF Grant DMR8819860. J.F.M. thanks the Fannie and John Hertz Foundation for a fellowship.

### Appendix

For the case of the angelellite stoichiometry but containing octahedral iron and five-coordinate arsenic the same method may be used as for the four-coordinate case. The electrostatic bond strength of an octahedral leg is as before  $3/6 = 1/2$ , but that for the trigonal bipyramidal arsenic is  $5/5 = 1$ . For the case where  $x$  octahedra and  $y$  trigonal bipyramids meet at an oxygen the electrostatic bond strength is  $x(1/2) + y(1) = 2$  or

$$x + 2y = 4 \quad (1A)$$

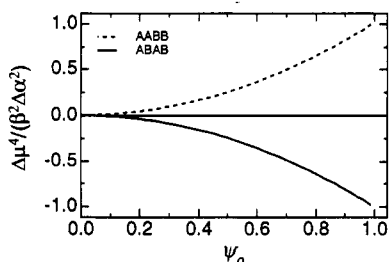
Since  $2y$  and  $4$  are even,  $x$  must be so too. The possible nonnegative integral solutions are then (i)  $x = 0, y = 2$ , (ii)  $x = 2, y = 1$ , and (iii)  $x = 4, y = 0$ . These correspond to the three cases: (i) a bond between two trigonal bipyramids; (ii) an oxygen linking two octahedra and one trigonal bipyramid; (iii) an oxygen linking four octahedra. In case iii,  $y = 0$ , and in case i,  $x = 0$ , so to ensure that both arsenic and iron are coordinated by oxygen, all structures must contain some oxygen atoms of type ii. In principle it is possible to build structures with such characteristics, a result in contrast to the one found above for arsenic tetrahedra.

(24) Burdett, J. K. *J. Solid State Chem.* 1982, 45, 399.



Table 5. Moments of ...AABB... Chain as a Function of Order Parameter

$i$	$\mu^i(\psi_0)$
1	$\alpha_A + \alpha_B$
2	$\alpha_A^2 + \alpha_B^2 + 1 / 2(1 + \psi_0^2)(\beta_{AA}^2 + \beta_{BB}^2) + (3 - \psi_0^2)\beta_{AB}^2$
3	$\alpha_A^3 + \alpha_B^3 + 3 / 2(1 + \psi_0^2)(\alpha_A\beta_{AA}^2 + \alpha_B\beta_{BB}^2) + 3 / 2\beta_{AB}^2(3 - \psi_0^2)(\alpha_A + \alpha_B)$
4	$\alpha_A^4 + \alpha_B^4 + 1 / 2(1 + \psi_0^2)(\beta_{AA}^4 + \beta_{BB}^4) + 3(1 + \psi_0^2)(\alpha_A^2\beta_{AA}^2 + \alpha_B^2\beta_{BB}^2) + \beta_{AB}^4(7 - 5\psi_0^2) + 2\beta_{AB}^2(3 - \psi_0^2)(\alpha_A^2 + \alpha_B^2 + \alpha_A\alpha_B) + 2\beta_{AB}^2(1 + \psi_0^2)(\beta_{AA}^2 + \beta_{BB}^2)$

Figure 9.  $\Delta\mu^i(\psi_0)$ ,  $i = 4$ , as a function of  $\psi_0$ . The structures are fully ordered at  $\psi_0 = 1$ .

It is worthwhile to see what topological arguments have to say further about this problem. The arguments are simple ones but a little tedious to describe. We first note that the stoichiometry requires that there be twice as many octahedra as trigonal bipyramids and, for every four octahedra and two trigonal bipyramids, 11 oxygen atoms and so we must consider too the constraints imposed on the octahedral network by this octahedra/trigonal bipyramid ratio. First consider the case where there is no bonding between the trigonal bipyramids. From the solutions of eq 4 a vertex of a trigonal bipyramid can then only be linked to a pair of octahedra (case ii,  $x = 2$ ,  $y = 1$ ). Assuming that no trigonal bipyramid shares an edge with any octahedron each trigonal bipyramid is thus bonded to five pairs, or 10 distinct, octahedra (one pair of octahedra at each of its five vertices). An octahedron has six vertices each of which is shared either with four octahedra or with two octahedra and one trigonal bipyramid. If  $n$  is the number of octahedral vertices connected to a trigonal bipyramid, and the ratio of octahedra to trigonal bipyramids is  $r$  ( $=2$  here), then from the connectivity of the network  $nr = 10$ . I.e., in order to maintain the balance of two octahedra to one trigonal bipyramid, it is required that five of the vertices belong to one trigonal bipyramid and to two octahedra. Thus each octahedron in the network has one 4-connected (to other octahedra) vertex and five 2-connected (to other octahedra) vertices. It is interesting to observe that this connectivity gives the correct number of oxygen atoms for the structure as a whole. Each formula unit contains four octahedra and two trigonal bipyramids. Since each oxygen belongs to an octahedron, counting the oxygen atoms which belong to the octahedral network will count all of the oxygen atoms. An octahedron has one 4-connected

(to other octahedra) vertex which contributes  $1/4$  oxygen and five 2-connected (to other octahedra) vertices each contributing  $1/2$  oxygen. This gives  $1/4 + 5/2$  oxygen/octahedron or  $4(1/4 + 5/2) = 11$  oxygens for four octahedra. This works generally for this problem. Once the appropriate proportion of vertices of each coordination to achieve the proper ratio of octahedra and trigonal bipyramids is arrived at, the network is found to also have the correct number of oxygen, a result which stems from the assignment of iron and arsenic valences at the beginning.

The case where trigonal bipyramids share vertices can be studied in the same way. The simplest situation is that where each trigonal bipyramid shares a single vertex with another trigonal bipyramid and four vertices with a pair of octahedra. If  $n$  is the number of octahedral vertices common to trigonal bipyramids, then using the connectivity argument from above,  $nr = 8$  or  $n = 4$ . This restriction requires that an octahedron have four vertices which are 2-connected (to other octahedra) and two which are 4-connected (to other octahedra). Now each pair of trigonal bipyramids contributes a single shared oxygen giving (for a formula unit of four octahedra and two trigonal bipyramids)  $4(2/4 + 4/2) + 2(1/2) = 11$  oxygen atoms. For the case where each trigonal bipyramid shares two vertices with other trigonal bipyramids and three vertices with octahedra, analogous arguments show that each octahedron needs to have three 2-connected (to other octahedra) and three 4-connected (to other octahedra) vertices. As the linked trigonal bipyramids now contribute two oxygen atoms the number of oxygens for a formula unit consisting of four octahedra and two trigonal bipyramids is as follows:  $4(3/4 + 3/2) + 2(2/2) = 11$ . It should be clear that there is a whole series of possibilities here controlled by the relationship  $nr = 2(5 - m)$  where  $m$  is the number of trigonal bipyramidal vertices shared with other trigonal bipyramids. Since  $r = 2$ , the number of vertices of each octahedron shared with trigonal bipyramids is just the same as the number of vertices shared by one trigonal bipyramid with another.

We have built structures for the case of  $m = 0$  which geometrically are quite feasible. Increasing the coordination around the arsenic atom compared to the observed angelellite structure leads to both an increase in the oxygen coordination number and in second-nearest neighbor coordination around the iron atom. We find a second-nearest neighbor coordination number of 9 compared to 7 in the observed structure.